View metadata, citation and similar papers at core.ac.uk

brought to you by CORE

provided by Elsevier - Publisher Connector

© 2006 International Society of Nephrology

Plasminogen activator inhibitor-1 deficiency protects against aldosterone-induced glomerular injury

J Ma[1], A Weisberg[2], JP Griffin[2], DE Vaughan[3], AB Fogo[4] and NJ Brown[2]

[1]*Division of Pediatric Nephrology, Department of Pediatrics, Vanderbilt University Medical Center, Nashville, Tennessee, USA;*
[2]*Division of Clinical Pharmacology, Department of Medicine, Vanderbilt University Medical Center, Nashville, Tennessee, USA;*
[3]*Division of Cardiovascular Medicine, Department of Medicine, Vanderbilt University Medical Center, Nashville, Tennessee, USA and*
[4]*Department of Pathology, Vanderbilt University Medical Center, Nashville, Tennessee, USA*

This study tests the hypothesis that plasminogen activator inhibitor-1 (PAI-1) contributes to aldosterone-induced renal and cardiac injury. The effects of 12-week aldosterone (2.8 μg/day)/salt (1% drinking water) versus vehicle/salt on renal and cardiac histology and mRNA expression were determined in wild-type (WT) and PAI-1 deficient (*PAI-1*$^{(-/-)}$) mice. Systolic blood pressure was similar in aldosterone-infused WT and *PAI-1*$^{(-/-)}$ mice until 12 weeks, when it was significantly higher in the WT mice. At 12 weeks, urine volume, sodium excretion, and sodium/potassium ratio were similarly increased in the two aldosterone-infused groups. In contrast, urine albumin excretion was greater in aldosterone-infused WT mice (mean $\pm$ s.d.: 699.0 $\pm$ 873.0 μg/24 h) compared to vehicle-infused WT (23.6 $\pm$ 9.0 μg/24 h, $P = 0.003$) or aldosterone-infused *PAI-1*$^{(-/-)}$ mice (131.6 $\pm$ 110.6 μg/24 h, $P = 0.007$). Aldosterone increased glomerular area to a greater extent in WT (4651 $\pm$ 577 versus 3278 $\pm$ 488 μm^2/glomerulus in vehicle-infused WT, $P < 0.001$) than in *PAI-1*$^{(-/-)}$ mice (3713 $\pm$ 705 μm^2/glomerulus, $P = 0.001$ versus aldosterone-infused WT), with corresponding mesangial expansion. Renal collagen content was also increased in aldosterone-infused WT versus *PAI-1*$^{(-/-)}$ mice. In WT mice, aldosterone increased renal mRNA expression of PAI-1, collagen I, collagen III, osteopontin, fibronectin, monocyte chemoattractant protein-1 (MCP-1), and F4/80 (all $P < 0.05$), but not transforming growth factor beta (TGF-β). In *PAI-1*$^{(-/-)}$ mice, aldosterone increased renal expression of collagen I, osteopontin, fibronectin, and MCP-1, and tended to increase collagen III. Renal osteopontin expression was diminished in aldosterone-treated *PAI-1*$^{(-/-)}$ compared to aldosterone-treated WT mice ($P = 0.05$). Aldosterone induced cardiac hypertrophy but not fibrosis in WT and *PAI-1*$^{(-/-)}$ mice. PAI-1 contributes to aldosterone-induced glomerular injury.

Correspondence: *NJ Brown, Division of Clinical Pharmacology, Department of Medicine, Vanderbilt University Medical Center, 560 Robinson Research Building, Nashville, Tennessee 37232-6602, USA. E-mail: nancy.j.brown@vanderbilt.edu*

Received 5 July 2005; revised 7 October 2005; accepted 28 October 2005; published online 8 February 2006

Kidney International (2006) **69,** 1064–1072. doi:10.1038/sj.ki.5000201; published online 8 February 2006

KEYWORDS: aldosterone; plasminogen activator inhibitor-1; angiotensin

The last several years have seen a paradigm shift in our understanding of how aldosterone contributes to cardiovascular and renal injury. Whereas it was once thought that aldosterone acts primarily as a circulating hormone involved in the regulation of sodium excretion through mineralocorticoid receptor (MR)-dependent mechanisms, studies now provide evidence for local, extra-adrenal production of aldosterone, as well as for extra-renal actions of aldosterone.[1] Aldosterone contributes to inflammatory and fibrotic effects that were previously attributed solely to angiotensin (Ang) II.[2–4] In clinical studies, MR antagonism has been shown to decrease mortality in patients with congestive heart failure,[5,6] to improve endothelial function,[7] to reduce circulating markers of collagen turnover,[8] and to decrease microalbuminuria.[9–13]

In rats, studies have consistently demonstrated that aldosterone causes cardiac hypertrophy and fibrosis through an MR-dependent pathway in the setting of high salt intake.[14–17] Similarly, aldosterone causes inflammation and fibrosis and glomerular injury in the kidney in hypertensive rats.[2,17–19] In these models, aldosterone induces cellular infiltration and the expression of inflammatory markers such as cyclooxygenase (COX)-2, ED-1 (rat monocyte/macrophage marker), interleukins, and osteopontin prior to the development of fibrosis.[4,18] However, the mechanism(s) involved in the progression from inflammation to fibrosis has not been delineated.

One possible mechanism through which aldosterone may promote the development of fibrosis is through induction of plasminogen activator inhibitor-1 (PAI-1) expression. Aldosterone induces PAI-1 expression in vascular smooth muscle cells and endothelial cells,[20] cardiomyocytes, and monocytes,[21] whereas MR antagonism decreases PAI-1 expression in the heart of Ang II/N^G-nitro-L-arginine methyl ester (L-NAME)-treated mice[22] and in the rat kidney following radiation injury or streptozotocin treatment.[23,24] PAI-1, a

principal inhibitor of plasminogen activators, can promote fibrosis by preventing the activation of matrix metalloproteinases (MMPs) and the degradation of extracellular matrix (ECM) by plasminogen activators and plasmin.[25] Studies using PAI-1-deficient or -overexpressing animals have implicated PAI-1 in the pathogenesis of bleomycin-induced pulmonary fibrosis,[26] perivascular fibrosis following nitric oxide synthase inhibition,[27] and renal fibrosis following unilateral ureteral obstruction.[28]

The present study tests the hypothesis that PAI-1 contributes to aldosterone-induced cardiac and renal injury. To do this, we determined the effect of aldosterone/salt administration in uninephrectomized wild-type (WT) and PAI-1-deficient animals.

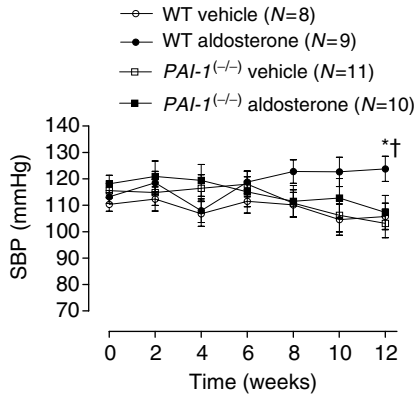

Figure 1 | Effect of vehicle and aldosterone infusion on systolic blood pressure (SBP) in wild-type (WT) and plasminogen activator inhibitor-1 (*PAI-1* $^{(-/-)}$) mice. $^{*}P = 0.025$ versus vehicle-infused wild-type, $^{\dagger}P = 0.007$ versus aldosterone-infused *PAI-1*$^{(-/-)}$.

RESULTS

Hemodynamic effects

Figure 1 shows systolic blood pressure (SBP) in each of the four treatment groups. SBP did not change significantly over the 12 weeks of the study in any of the treatment groups and was not significantly different among the study groups over the entire period of the study (mean SBP 108.3 ± 9.0, 116.9 ± 9.0, 113.2 ± 9.0, and 112.6 ± 9.0 mmHg in vehicle-infused WT, aldosterone-infused WT, vehicle-infused *PAI-1*$^{(-/-)}$, and aldosterone-infused *PAI-1*$^{(-/-)}$ mice, respectively, $P = 0.160$) However, SBP was significantly higher at 12 weeks in aldosterone-infused WT compared to either vehicle-infused WT ($P = 0.025$) or aldosterone-infused *PAI-1*$^{(-/-)}$ mice ($P = 0.007$).

Renal function

As illustrated in Table 1, plasma aldosterone concentrations were significantly and similarly increased in either group of aldosterone-infused mice compared to vehicle-infused mice. Glucose concentrations were similar among the treatment groups at all time points. Baseline urine volume, sodium or potassium excretion, and albumin excretion were similar among treatment groups, while baseline urine sodium/potassium ratio was mildly but significantly increased in *PAI-1*$^{(-/-)}$ mice. At 12 weeks, water consumption (not shown) and urine volume, as well as urine sodium excretion and the urine sodium/potassium ratio were significantly increased in the two aldosterone-infused groups. There was no difference in any of these parameters between aldosterone-infused WT and *PAI-1*$^{(-/-)}$ mice. In contrast, urine protein excretion, as measured by either the albumin/creatinine ratio or 24-h albumin excretion, was significantly increased in aldosterone-infused WT mice compared to either vehicle-infused mice or to aldosterone-infused *PAI-1*$^{(-/-)}$ mice.

Renal histology

Body weights were similar at 12 weeks among all four treatment groups (Table 2). The kidney/body weight ratio was significantly increased in aldosterone-infused WT and *PAI-1*$^{(-/-)}$ mice compared to vehicle-infused mice and this effect was significantly greater in the aldosterone-infused WT mice ($P < 0.05$). The kidneys of both aldosterone-infused WT and *PAI-1*$^{(-/-)}$ mice demonstrated marked collecting duct dilatation, associated with focal hyperplasia and hypertrophy, a lesion not found in vehicle-treated mice (Figure 2). Compared to the kidneys of vehicle-infused mice, the kidneys of aldosterone-infused mice were characterized by glomerular hypertrophy. However, glomerular area ($P = 0.001$, Table 2) and mesangial area ($P = 0.035$) were increased to a significantly greater extent in kidneys from aldosterone-infused WT mice compared to aldosterone-infused *PAI-1*$^{(-/-)}$ mice. Glomerular collagen IV content also tended to be increased in aldosterone-infused WT mice compared to aldosterone-infused *PAI-1*$^{(-/-)}$ mice ($P = 0.058$, Table 2). Aldosterone tended to induce interstitial fibrosis ($P = 0.071$ for treatment effect) but did not cause perivascular fibrosis in WT or *PAI-1*$^{(-/-)}$ mice. Total renal collagen content was increased in aldosterone-infused WT mice compared to aldosterone-infused *PAI-1*$^{(-/-)}$ ($P = 0.039$) or vehicle-infused WT ($P = 0.024$) mice. Renal plasmin activity was increased in vehicle-infused *PAI-1*$^{(-/-)}$ compared to vehicle-infused WT mice, but was similar in aldosterone-infused *PAI-1*$^{(-/-)}$ and WT mice (Table 2). However, MMP-2 activity was increased in vehicle-infused *PAI-1*$^{(-/-)}$ and increased further in aldosterone-infused *PAI-1*$^{(-/-)}$ mice, such that MMP-2 activity was higher in aldosterone-infused *PAI-1*$^{(-/-)}$ mice compared to WT mice.

F4/80-positive cells were detected in the renal interstitium but not in glomeruli (Table 2, Figure 3a–d). Compared to the kidneys of vehicle-infused WT mice, the kidneys of aldosterone-infused WT and *PAI-1*$^{(-/-)}$ mice showed significantly increased number of F4/80-positive cells, especially in areas of interstitial fibrosis and surrounding interlobular arteries and glomeruli. There was no significant difference in macrophage staining of aldosterone-infused *PAI-1*$^{(-/-)}$ mice compared to vehicle-infused *PAI-1*$^{(-/-)}$ mice. Interstitial fibrosis was increased in aldosterone-infused compared to vehicle-infused *PAI-1*$^{(-/-)}$ mice, but not compared to WT mice.

Table 1 | Metabolic and renal functional parameters in WT and *PAI-1*$^{(-/-)}$ mice

	WT		*PAI-1*$^{(-/-)}$	
	Vehicle (*N*=8)	Aldosterone (*N*=9)	Vehicle (*N*=11)	Aldosterone (*N*=10)
Aldosterone (pg/ml)				
Week 12	163.5±89.5	462.6±365.7*,†	166.2±141.4	600.4±455.7*,‡
Glucose (mg/dl)				
Week 0	161.5±12.0	157.7±14.6	160.6±15.2	154.6±25.2
Week 12	133.8±25.7	119.9±22.6	150.6±23.2	129.4±27.6
Urine volume (ml)				
Week 0	1.3±0.5	1.3±0.6	1.5±0.5	1.1±0.7
Week 12	4.0±1.1	21.9±10.1§,‖	4.7±2.9	21.8±17.8§,‖
Urine Na (μEq/day)				
Week 0	250±96	237±85	243±96	190±120
Week 12	1095±341	3371±1551¶,†	1551±624	4091±3354*,‖
Urine K (μEq/day)				
Week 0	632±191	511±182	511±229	384±279
Week 12	654±133	863±561	568±290	582±380
Urine Na/K ratio				
Week 0	0.39±0.07	0.47±0.08	0.52±0.14¶	0.59±0.16*
Week 12	1.67±0.29	4.20±1.61§,‡	2.03±0.34	7.62±8.20¶,‡
Urine albumin/creatinine ratio (μg/mg)				
Week 0	10.3±7.7	13.5±13.9	9.5±3.0	12.2±6.1
Week 12	22.9±7.4	167.9±190.2*,‖	21.9±9.7	35.8±14.3#
Urinary albumin excretion (μg/24 h)				
Week 0	7.8±3.5	10.8±8.6	7.8±2.5	5.6±3.2
Week 12	23.6±9.0	699.0±873.0*,‖	23.7±14.7	131.6±110.6**

PAI-1, plasminogen activator inhibitor-1; WT, wild type.
*$P \leqslant 0.005$ versus vehicle-infused wild-type mice, †$P < 0.05$ versus vehicle-infused *PAI-1*$^{(-/-)}$ mice, ‡$P \leqslant 0.005$ versus vehicle-infused *PAI-1*$^{(-/-)}$ mice, §$P \leqslant 0.001$ versus vehicle-infused wild-type mice, ‖$P < 0.001$ versus vehicle-infused *PAI-1*$^{(-/-)}$ mice, ¶$P < 0.05$ versus vehicle-infused wild-type mice, #$P < 0.005$ versus aldosterone-infused wild-type mice, **$P < 0.01$ versus aldosterone-infused wild-type mice.

Table 2 | Renal morphology and histology in WT and *PAI-1*$^{(-/-)}$ mice

	WT		*PAI-1*$^{(-/-)}$	
	Vehicle (*N*=8)	Aldosterone (*N*=9)	Vehicle (*N*=11)	Aldosterone (*N*=10)
Body weight (g)	26.5±1.0	28.5±2.4	27.1±1.7	27.5±2.3
Kidney weight/body weight (mg/g)	9.66±0.55	13.39±1.17*,†	8.66±0.60	12.14±2.16*,†,‡
Glomerular area (μm^2/glomerulus)	3278±488	4652±577*,†	2953±513	3713±705§,‖
Glomerular mesangial area (points/glomerulus)	7.66±1.41	10.50±2.67¶,†	6.22±0.73	8.02±1.72
Glomerular collagen IV area (μm^2)	712±166	1335±359*,†	750±242	1079±319§,¶
Renal interstitial fibrosis score	0.13±0.35	0.67±1.00	0.09±0.30	0.78±0.83§
Macrophage infiltration score	0±0	1.44±1.01*,§	0.54±0.82	1.22±0.67#
Renal collagen content (mg/g)	3.4±1.0	6.3±3.2¶	4.2±0.5	3.5±1.4‡
Glomerular PSmad2 staining score	1.4±0.9	2.7±1.3	1.8±0.8	2.3±1.3
Tubular PSmad2 staining score	3.2±1.6	2.6±0.5	2.6±1.1	4.5±1.3‡,§
Renal plasmin activity (mU/mg)	0.21±0.16	0.62±0.31	0.63±0.69*	0.56±0.23
MMP-2 activity	0.28±0.10	0.75±0.17*	0.70±0.16*	1.03±0.31*,‡,§
MMP-9 activity	3.00±0.82	3.87±1.01	4.99±1.79#	4.07±0.99

MMP, matrix metalloproteinases; PAI-1, plasminogen activator inhibitor-1; WT, wild type.
*$P < 0.001$ versus vehicle-infused wild-type mice, †$P \leqslant 0.001$ versus vehicle-infused *PAI-1*$^{(-/-)}$, ‡$P < 0.05$ versus aldosterone-infused wild-type mice, §$P < 0.05$ versus vehicle-infused *PAI-1*$^{(-/-)}$, ‖$P = 0.001$ versus aldosterone-infused wild-type, ¶$P < 0.05$ versus vehicle-infused wild-type, #$P < 0.005$ versus vehicle-infused wild-type.

Cardiac function and cardiac and aortic histology

Heart weight/body weight was significantly and similarly increased in the two aldosterone-infused groups (Table 3). Likewise, aldosterone induced comparable aortic medial hypertrophy in the WT and *PAI-1*$^{(-/-)}$ mice. On the other hand, aldosterone increased some measures of left ventricular hypertrophy (LVFT at autopsy and interventricular septum in systole (IVSs) on echocardiography) to a greater extent in

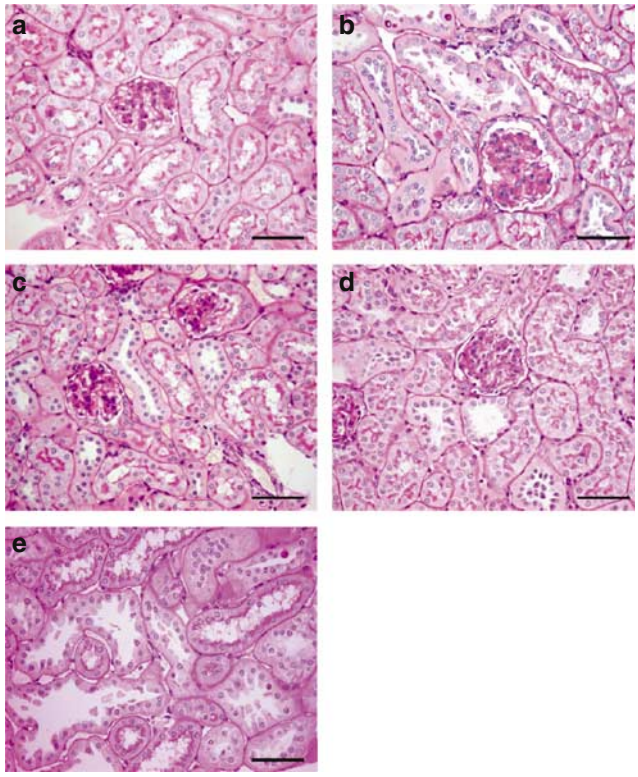

Figure 2 | Renal histological changes in wild-type and *PAI-1*$^{(-/-)}$ mice given aldosterone and 1% NaCl after uninephrectomy. Glomeruli were enlarged with mesangial expansion in kidneys from (**b**) aldosterone-infused wild-type mice versus (**a**) those from wild-type mice infused with vehicle and (**d**) those from *PAI-1*$^{(-/-)}$ mice infused with aldosterone. (**c**) Comparison between the vehicle- and (**d**) aldosterone-infused *PAI-1*$^{(-/-)}$ kidneys suggests that PAI-1 deficiency protected against aldosterone-induced damage in this model. Aldosterone infusion also caused remarkable dilatation, hypertrophy, and hyperplasia of renal collecting tubules in both WT and *PAI-1*$^{(-/-)}$ kidneys with occasional calcium deposits (**e**). Bar = 100 μm (periodic acid-Schiff).

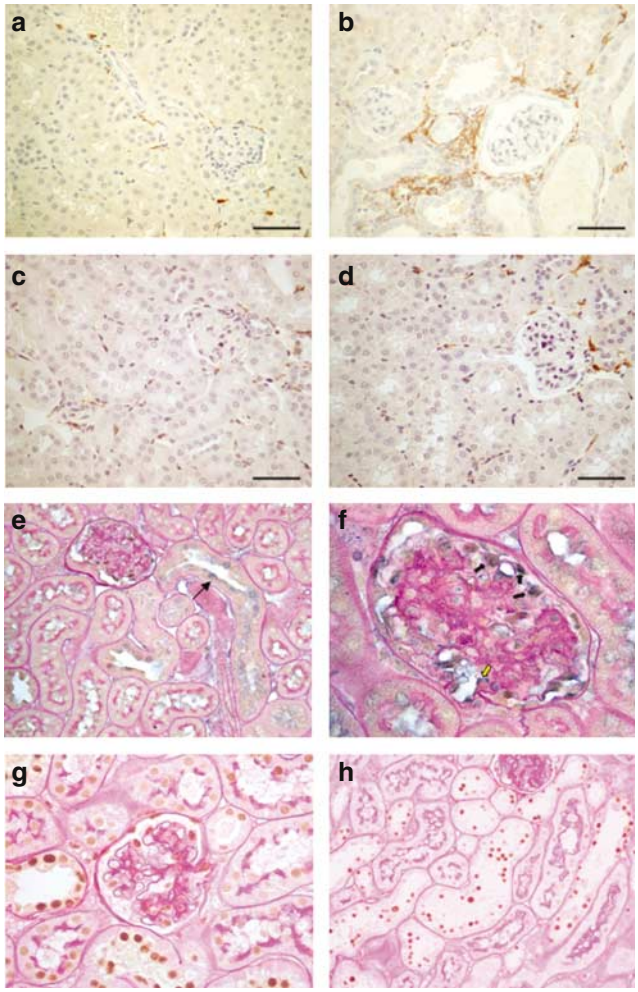

Figure 3 | Renal macrophage infiltration in wild-type and *PAI-1*$^{(-/-)}$ mice given aldosterone and 1% NaCl after uninephrectomy. There was scattered infiltration of macrophages in the renal interstitium in both vehicle-infused (**a**) wild-type and (**c**) *PAI-1*$^{(-/-)}$ mice. F4/80-positive macrophages were increased in the interstitium of kidneys from (**b**) wild-type and (**d**) *PAI-1* $^{(-/-)}$ mice infused with aldosterone. Bar = 100 μm (antibody to F4/80). (**e**) Osteopontin mRNA signal (blue–purple) was detected in the collecting tubules (arrow) of aldosterone-treated WT mice. (**f**) In glomeruli of aldosterone-infused WT mice, osteopontin mRNA signal was detected on podocytes (black arrows) stained with WT-1 (brown) and capillary loop, consistent with endothelial cells (yellow arrow). Immunohistochemistry for PSmad2 (brown) showed increased staining in the (**g**) glomeruli of aldosterone-infused WT mice and (**h**) the tubules of aldosterone-infused *PAI-1*$^{(-/-)}$ mice.

WT mice than in *PAI-1*$^{(-/-)}$ mice. Likewise, aldosterone infusion was associated with an increase in estimated left ventricular mass (LVMd)/body weight measured by echocardiography in WT, but not in *PAI-1*$^{(-/-)}$ mice. Fractional shortening was significantly greater in either vehicle- and aldosterone-infused *PAI-1*$^{(-/-)}$ mice compared to WT mice. Aldosterone did not induce significant cardiac fibrosis (Table 3, $P = 0.324$), F4/80 staining (data not shown), or aortic medial fibrosis in WT or *PAI-1*$^{(-/-)}$ mice.

Renal gene expression

In WT mice, aldosterone increased the renal mRNA expression of PAI-1, collagen I, collagen III, osteopontin, fibronectin, monocyte chemoattractant protein-1 (MCP-1), and F4/80, but not transforming growth factor beta (TGF-β) compared to vehicle infusion (Figure 4). As expected, there was no significant PAI-1 expression in *PAI-1*$^{(-/-)}$ mice. In *PAI-1*$^{(-/-)}$ mice, aldosterone induced increased renal mRNA expression of collagen I, osteopontin, fibronectin, and MCP-1 and tended to increase expression of collagen III ($P = 0.078$), but not F4/80. Renal osteopontin expression was significantly decreased in aldosterone-infused *PAI-1*$^{(-/-)}$ animals compared to aldosterone-infused WT mice. Osteopontin expression correlated significantly with glomerular area (Spearman's correlation coefficient 0.534, $P = 0.002$) and the urine albumin/creatinine ratio (correlation coefficient 0.810, $P < 0.001$). By *in situ* hybridization, osteopontin mRNA signal localized to the tubules and to capillary loops, consistent with endothelial cells, and to podocytes within

Table 3 | Cardiac and aortic morphology and echocardiographic measurements in WT and *PAI-1*$^{(-/-)}$ mice

	WT		*PAI-1*$^{(-/-)}$	
	Vehicle (*N*=8)	Aldosterone (*N*=9)	Vehicle (*N*=11)	Aldosterone (*N*=10)
Heart weight/body weight (mg/g)	4.94±0.26	5.98±0.76*,†	5.03±0.52	6.71±1.62‡,§
Left ventricular free wall (μm)	543.4±226.9	790.0±250.0‖,¶	555.4±85.7	678.7±121.4
Fibrosis score	0.81±0.37	1.06±0.53	0.86±0.32	1.17±0.56
PSmad2-positive cells/HPF	78.3±17.5	74.7±21.2	80.6±16.4	98.1±43.5
Aortic media (μm)	48.07±8.18	62.65±12.41‖,§	45.68±7.45	64.70±12.08‖,§
Aortic adventia (μm)	30.8±8.7	36.4±15.0	33.8±7.2	42.9±12.1
Echocardiography				
IVSd (cm)	0.097±0.004	0.109±0.014	0.100±0.008	0.101±0.009
LVIDd (cm)	0.280±0.026	0.306±0.040	0.271±0.024	0.297±0.041
LVPWd (cm)	0.092±0.009	0.106±0.009*,†	0.093±0.011	0.100±0.016
IVSs (cm)	0.175±0.014	0.193±0.020*	0.180±0.011	0.173±0.017#
LVIDs (cm)	0.144±0.021	0.157±0.026¶	0.123±0.012	0.148±0.035†
LVPWs (cm)	0.119±0.015	0.133±0.018	0.121±0.019	0.137±0.030
FS (%)	48.6±5.6	48.9±2.7	54.5±1.8‖,**	50.7±5.1†
HR (b.p.m.)	733±32	723±16	713±18	684±80
LVMd (g)	0.086±0.012	0.121±0.031‖,¶	0.085±0.017	0.104±0.030
LVMd/BW (mg/g)	3.2±0.5	4.2±0.9*,¶	3.0±0.6	3.8±1.2†

BW, body weight; d, diastolic; FS, fractional shortening; HR, heart rate; HPF, high power field; IVS, interventricular septum; LV, left ventricular; LVID, LV internal dimension; LVM, LV mass; LVPW, LV posterior wall; PAI-1, plasminogen activator inhibitor-1; s, systolic; WT, wild type.
*$P<0.05$ versus vehicle-infused wild-type mice, †$P<0.05$ versus vehicle-infused *PAI-1*$^{(-/-)}$ mice, ‡$P<0.001$ versus vehicle-infused wild-type, §$P\leqslant0.001$ versus vehicle-infused *PAI-1*$^{(-/-)}$, ‖$P<0.01$ versus vehicle-infused wild-type, ¶$P<0.01$ versus vehicle-infused *PAI-1*$^{(-/-)}$, #$P<0.05$ versus aldosterone-infused wild-type mice, **$P<0.005$ versus aldosterone-infused wild-type mice.

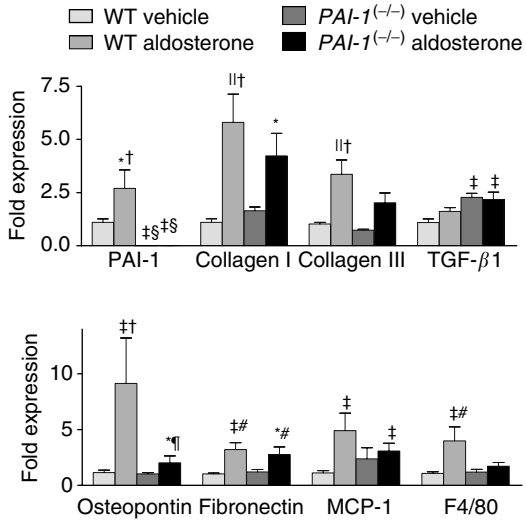

Figure 4 | Effect of aldosterone treatment on renal gene expression in wild-type (WT) and plasminogen activator inhibitor-1 *(PAI-1)* $^{(-/-)}$ mice. *N* was 5 or more per group. *$P\leqslant0.05$ versus vehicle-infused WT, †$P\leqslant0.001$ versus vehicle-infused *PAI-1*$^{(-/-)}$, ‡$P\leqslant0.008$ versus vehicle-infused WT, §$P<0.005$ versus aldosterone-infused WT, ‖$P<0.001$ versus vehicle-infused WT, ¶$P<0.05$ versus aldosterone-infused WT, #$P<0.05$ versus vehicle-infused *PAI-1*$^{(-/-)}$.

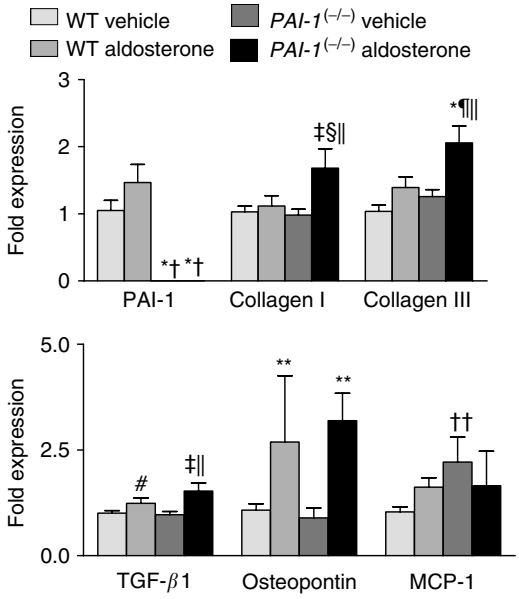

Figure 5 | Effect of aldosterone treatment on cardiac gene expression in wild-type (WT) and plasminogen activator inhibitor-1 *(PAI-1)* $^{(-/-)}$ mice. *N* was 5 or more per group. *$P<0.001$ versus vehicle-infused WT mice, †$P<0.001$ versus aldosterone-infused WT mice, ‡$P<0.01$ versus vehicle-infused WT mice, §$P<0.05$ versus aldosterone-infused WT mice, ‖$P<0.01$ versus vehicle-infused *PAI-1*$^{(-/-)}$ mice, ¶$P<0.01$ versus aldosterone-infused WT mice, #$P<0.05$ versus vehicle-infused *PAI-1*$^{(-/-)}$ mice, **$P<0.05$ versus either vehicle-infused groups, ††$P<0.05$ versus vehicle-infused WT.

glomeruli (Figure 3e and f). TGF-β expression was significantly increased in the kidney of both vehicle- and aldosterone-infused *PAI-1*$^{(-/-)}$ mice compared to vehicle-infused WT mice. Phospho-Smad2 (PSmad2) staining tended to be increased in the glomeruli of aldosterone-infused WT mice, whereas tubular PSmad2 tended to be increased in aldosterone-infused *PAI-1*$^{(-/-)}$ mice (Table 2 and Figure 3g and h).

Cardiac gene expression

Figure 5 shows the effect of aldosterone treatment on cardiac gene expression in WT and *PAI-1*$^{(-/-)}$ mice. Although aldosterone tended to increase cardiac PAI-1 expression in

WT mice, this effect was not significant ($P = 0.093$). Aldosterone increased cardiac osteopontin expression in WT or *PAI-1*$^{(-/-)}$ mice ($P = 0.019$ for an overall effect of aldosterone) but, in contrast to the kidney, cardiac osteopontin expression was similar in aldosterone-infused WT and *PAI-1*$^{(-/-)}$ mice. Moreover, aldosterone induced cardiac expression of collagen I and III and TGF-β in *PAI-1*$^{(-/-)}$ mice but not in WT mice. However, the number of PSmad2-positive cells in the heart was similar among all of the treatment groups. Because there were no morphological or histological differences between the aortas of aldosterone-infused WT and *PAI-1*$^{(-/-)}$ mice, we did not determine aortic gene expression.

DISCUSSION

Aldosterone causes glomerular injury in animal models, whereas MR antagonism reduces proteinuria and glomerular sclerosis in hypertensive rats.[2,17–19] MR antagonism also reduces urinary albumin excretion in patients with hypertensive or diabetic nephropathy.[9–13] At the same time, PAI-1 has been implicated in animal models of interstitial fibrosis and glomerulosclerosis, including ureteral obstruction-induced interstitial fibrosis, crescentic glomerulonephritis, anti-Thy-1 glomerulonephritis, and diabetic nephropathy.[28–32] Experimental data indicating that aldosterone induces PAI-1 expression *in vitro*,[20,21] and that MR antagonism reduces glomerular PAI-1 expression and sclerosis *in vivo*,[23,24] suggested the hypothesis that aldosterone induces glomerular injury, in part, by enhancing PAI-1 expression. The present study addresses this hypothesis and indicates that genetic PAI-1 deficiency protects against aldosterone-induced glomerular injury, as measured histologically by glomerular and mesangial expansion and functionally by albumin excretion.

In both WT and *PAI-1*$^{(-/-)}$ mice, aldosterone/salt increased urine volume, sodium excretion, and urine sodium-to-potassium ratio, consistent with increased consumption of saline, as well as with the 'aldosterone-escape' phenomenon whereby the kidney overcomes aldosterone-mediated tubular NaCl reabsorption in the setting of normo- or hypervolemia, most likely through a decrease in the thiazide-sensitive NaCl cotransporter of the distal convoluted tubule.[33] Similarly, aldosterone caused renal tubular dilatation in both WT and *PAI-1*$^{(-/-)}$ mice, described previously in transgenic mice overexpressing the human MR.[34] PAI-1 deficiency also did not affect aldosterone-induced interstitial inflammation. In contrast, PAI-1 deficiency attenuated aldosterone-induced glomerular injury despite similar aldosterone concentrations, potassium and sodium excretion, and glucose concentrations in WT and *PAI-1*$^{(-/-)}$ mice.

PAI-1 deficiency could protect against glomerular injury via decreased ECM formation or increased degradation. As in unilateral ureteral observation-induced interstitial fibrosis,[28] PAI-1 deficiency was not associated with enhanced renal plasmin activity during aldosterone treatment. Likewise, aldosterone induced statistically similar increases in renal collagen and fibronectin expression in WT and *PAI-1*$^{(-/-)}$ mice. Taken together with the finding that total renal collagen content and intraglomerular collagen IV were decreased in aldosterone-infused *PAI-1*$^{(-/-)}$ mice compared to WT mice, the data are compatible with enhanced ECM degradation in the aldosterone-treated *PAI-1*$^{(-/-)}$ mice via a plasmin-independent pathway, possibly via increased activity of MMP-2.

It is not possible to exclude a blood pressure-dependent protective effect of PAI-1 deficiency on aldosterone-induced renal injury with certainty. On the one hand, SBP was similar among the groups until the end of the study and the degree of cardiac and aortic medial hypertrophy was similar in the aldosterone-infused WT and *PAI-1*$^{(-/-)}$ mice at autopsy. On the other hand, SBP was higher in the aldosterone-infused WT mice relative to the *PAI-1*$^{(-/-)}$ mice at the last week of the study and some echocardiographic measures of left ventricular hypertrophy imply a greater pressor stimulus in the aldosterone-infused WT mice compared to the aldosterone-infused *PAI-1*$^{(-/-)}$ mice. However, the fact that blood pressure diverged only late in the study suggests that this difference in blood pressure was a consequence of, rather than a cause of, glomerular injury.

As reported previously in Sprague–Dawley rats,[18] aldosterone significantly increased renal expression of the inflammatory marker genes osteopontin, MCP-1, and F4/80. Importantly, in *PAI-1*$^{(-/-)}$ mice, attenuation of glomerular injury was associated with decreased osteopontin expression. Further studies are needed to investigate the interaction between PAI-1 and osteopontin expression in the kidney. However, binding to integrin ligands such as collagen I and fibronectin induces osteopontin expression in osteoblastic cells.[35] If adhesion to integrins similarly stimulates podocyte osteopontin expression, PAI-1 deficiency could alter osteopontin expression by enhancing degradation of collagen and fibronectin.

Significantly, aldosterone/salt treatment did not increase TGF-β expression in the kidney. This is compatible with prior data in $\beta 6^{(-/-)}$ mice indicating that aldosterone can induce renal PAI-1 expression and fibrosis through a TGF-β-independent pathway.[36] Surprisingly, however, renal mRNA expression of TGF-β was increased in *PAI-1*$^{(-/-)}$ versus WT mice in the presence or absence of aldosterone. Based on PSmad2 staining, active TGF-β was also increased in the tubules of aldosterone/salt-treated *PAI-1*$^{(-/-)}$ mice. This may account for increased interstitial fibrosis in these mice compared to vehicle-treated *PAI-1*$^{(-/-)}$ mice. While it is known that TGF-β increases PAI-1 expression,[37] that plasmin activates TGF-β,[38] and that PAI-1 deficiency can lead to activation of TGF-β,[39] to the best of our knowledge this is the first observation of increased TGF-β expression associated with PAI-1 deficiency. Rather, other groups have reported decreased TGF-β expression in injured *PAI-1*$^{(-/-)}$ mice;[28] however, a recent study in cultured mesangial cells suggests that the effect of PAI-1 on TGF-β expression may depend on

interactions with urokinase plasminogen activator and its receptor.[32]

Aldosterone/salt induced cardiac TGF-β expression in both WT and *PAI-1*$^{(-/-)}$ mice; increased TGF-β expression could have contributed to the development of hypertrophy.[40] However, aldosterone/salt did not induce cardiac fibrosis in the current study, contrary to the profibrotic effect of aldosterone/salt observed in rat models.[14–16] Similar findings in other studies in mice[22,41] suggest that there may be species differences in susceptibility to Ang II or aldosterone/salt-induced cardiac fibrosis. In this regard, the minimal pressor response to aldosterone observed in the present study contrasts the 30–50 mmHg increase in blood pressure typically reported during chronic aldosterone/salt treatment in rats, despite comparable aldosterone doses on a per weight basis.[14,42] Given evidence that aldosterone/salt induces cardiac fibrosis in part through upregulation of the AT_1 receptor,[43,44] differences in susceptibility to fibrosis in rats and mice could reflect species differences in Ang II receptor regulation.[45]

Despite the lack of cardiac fibrosis in aldosterone-treated mice, PAI-1 deficiency interacted synergistically with aldosterone to induce cardiac expression of collagens I and III. These findings are compatible with the data of Oestreicher *et al.*,[22] who reported that PAI-1 deficiency increased inflammation induced by 2-week hypertensive treatment with Ang II and the nitric oxide synthase inhibitor L-NAME. Similarly, pharmacological PAI-1 inhibition and genetic PAI-1 deficiency promote Ang II-induced cardiac fibrosis.[46] The divergent effects of PAI-1 deficiency on the expression of profibrotic genes in the heart and the kidney may reflect different roles for PAI-1 in these two organs.[47] While PAI-1 promotes ECM accumulation by inhibiting MMP activation and retarding ECM turnover (as in the glomerulus), PAI-1 can retard inflammation and fibrosis by impeding urokinase plasminogen activator or plasmin-mediated activation or release of latent growth factors. If during PAI-1 deficiency, urokinase plasminogen activator or plasmin-mediated activation of growth factors exceeds degradation of ECM, fibrosis will result. Consistent with this hypothesis, excess cardiac fibrosis has been reported in aged PAI-1-deficient mice and in mice overexpressing macrophage urokinase plasminogen activator.[48]

In summary, aldosterone/salt induced glomerular hypertrophy and injury, as well as cardiac and aortic hypertrophy in this mouse model. PAI-1 deficiency protected against both aldosterone/salt-induced glomerular hypertrophy and injury, but not against macrophage infiltration, interstitial fibrosis, or activation of tubular TGF-β. PAI-1 deficiency did not affect cardiac and aortic hypertrophy and increased the cardiac expression of profibrotic genes. These findings have important implications for the treatment of aldosterone-dependent renal disease, and suggest site-specific differential interactions of aldosterone/salt and PAI-1. MR antagonism reduces urinary albumin excretion in patients with hypertensive or diabetic nephropathy.[9–13] Therapeutic strategies to reduce PAI-1 production or activity may be of value in preventing aldosterone-induced glomerular injury but may not reduce interstitial fibrosis.

MATERIALS AND METHODS

Animals

Adult male *PAI-1*$^{(-/-)}$ mice which had been backcrossed for eight generations on a C57BL/6J background (Jackson Laboratory, Bar Harbor, ME, USA) and C57BL/6J WT mice were studied. All animals were housed in a pathogen-free environment with a 12-h light/dark cycle and had free access to standard mouse chow and tap water until the initiation of the study. All animal procedures were approved by the Vanderbilt University Institutional Animal Care and Use Committee.

Protocol

After a 2–3-week training period for blood pressure measurements, 8- to 10-week-old mice were uninephrectomized under anesthesia with pentobarbital (50 mg/kg, i.p.) at week 0. At the same time, WT and *PAI-1*$^{(-/-)}$ mice were randomized to subcutaneous implantation of an osmotic mini-pump (Alzet model 2004, Alza Co., Palo Alto, CA, USA) containing either 0.467 μg/μl D-aldosterone (Sigma, St Louis, MO, USA) or vehicle (3.6% v:v dimethyl sulfoxide). Beginning at week 0, all mice were given drinking water containing 1% NaCl. At 4 and 8 weeks, pumps were explanted and a new pump was implanted under pentobarbital anesthesia. Thus, aldosterone-treated mice were given 2.8 μg aldosterone per day for 12 weeks.

SBP was measured using tail-cuff impedance plethysmography (BP-2000 Blood Pressure Analysis System, Visitech Systems, Apex, NC, USA) in trained unanesthetized mice prewarmed for 5–10 min at 37°C every 2 weeks. At week 0 and week 12, 24 h urine was collected in metabolic cages (Nalgene Co., Rochester, NY, USA). Because PAI-1 deficiency can decrease serum glucose concentrations,[49] 30 μl of blood was obtained from the saphenous vein for measurement of blood glucose at 0, 2, 4, 8, and 12 weeks. Mice were killed at week 12 by cervical dislocation. The renal artery was clamped and blood was drawn from the heart. The heart, the aorta, and the kidney were then harvested and the heart and kidney were weighed. The base of the heart, the first 2 mm of descending aorta, and coronal sections of the kidney were fixed in 4% buffered paraformaldehyde overnight and then processed and embedded in paraffin for histological evaluation. The remainder of the heart, aorta, and kidney were snap-frozen in liquid nitrogen for mRNA analysis.

Biochemical measurements

Urine sodium and potassium and serum potassium were measured by flame photometry. Urinary albumin, creatinine, and albumin/creatinine ratio were determined using a Bayer DCA2000 system (Elkhart, IN, USA). Blood glucose was measured using a HemoCue® (Ängelholm, Sweden) B-Glucose Analyzer. Aldosterone was measured using a commercially available radioimmunoassay (MP Biomedicals, Irvine, CA, USA). Hydroxyproline, measured by high-pressure liquid chromatography (HPLC) was used to assess the total collagen content in renal tissue from at least four mice per group. Renal plasmin activity was measured by chromogenic assay with a plasmin-specific chromogenic substrate, Chromozym PL (Boehringer Mannheim, Indianapolis, IN, USA),[28] and activities of MMP-2 and MMP-9 were examined by zymography on gelatin gels as described in detail online.[50]

Echocardiography

Transthoracic echocardiography was performed in conscious mice at week 11 using a 15-MHz transducer (Sonos 5500 system, Agilent, Andover, MA, USA).[51] Left ventricular wall thickness and chamber dimensions were determined from M-mode tracings, and the fractional shortening (FS%) and estimated left ventricular mass (LVM) were calculated as previously described. Heart rate (HR) was determined from the cardiac cycles recorded on the M-mode tracing using at least 10 consecutive beats.

Histology

All histological evaluation and morphometric analysis were performed in a blinded fashion. Four micrometer sections of paraffin-embedded kidney tissue were stained with periodic acid-Schiff. Glomerular morphometric analysis was performed using a $\times 40$ objective on at least 30 consecutive glomeruli and averaged for each animal. Glomerular area was measured by using KS300 Software (Kontron Electronic GmbH, Eching, Germany). A point-counting method was applied to assess glomerular mesangial volume. In total, 50 points were assessed for each glomerulus and the number of points falling exclusively on the mesangium was counted. Glomerular collagen content was semiquantified using KS300 Software on sections stained for collagen IV as described online.

Paraffin-embedded sections ($4\,\mu$m) of the heart and aorta were stained with Masson's trichrome. Free wall thickness of the left ventricle (LVFT) was measured under the $\times 10$ objective by using KS300 software. The thicknesses of media and adventitia of the aorta were measured on cross-sections with the $\times 20$ objective. Cardiac fibrosis was graded according to the presence or absence of subendocardial fibrosis (0.5), mild intra-cardiac fibrosis (1.0), moderate multi-focal intra-cardiac fibrosis (1.5), or multi-focal intra-cardiac fibrosis with perivascular extension (2). Aortic medial fibrosis was graded as absent (0), minimal focal (0.5), mild multi-focal (1), and moderate multi-focal (2).

Quantitative real-time PCR

Total RNA was extracted using RNAWiz (Ambion, Austin, TX, USA) and RNeasy Midi Kit (Qiagen, Valencia, CA, USA). Reverse transcription was performed using TaqMan Reverse Transcription Kit (Applied Biosystems, Branchburg, NJ, USA). Primers and conditions are available online. Experimental cycle threshold (C_t) values were normalized to β-actin measured on the same plate, and fold differences in gene expression were determined using the $2^{-\Delta\Delta C_t}$ method.[52]

Immunohistochemistry and *in situ* hybridization

Detailed methods for immunohistochemistry against F4/80 and PSmad2 appear online. F4/80-positive cells in the interstitium of the kidney were assessed by a macrophage infiltration score, with 0 indicating <20 positive cells in any high power field (HPF, $\times 40$), 1 indicating $\geqslant 20$ but <50 positive cells in any HPF, 2 indicating patchy moderate infiltrate with $\geqslant 50$ up to 100 positive cells in any HPF, and 3 indicating focal, patchy, severe infiltrate with $\geqslant 100$ positive cells in any HPF. PSmad2 staining was assessed in $\times 40$ HPFs and scored as 1–6 denoting >0 and $\leqslant 50$, >50 and $\leqslant 100$, >100 and $\leqslant 150$, >150 and $\leqslant 200$, >200 and $\leqslant 250$, >250 positive nuclei per HPF for tubules, while scored as 1– 5 denoting >0 and $\leqslant 5$, >5 and $\leqslant 10$, >10 and $\leqslant 15$, >15 and $\leqslant 20$, >20 positive nuclei per glomerulus for each animal. An average score was then calculated for each animal.

Statistical analysis

Results are expressed as mean $\pm$ s.d. in the text and tables and means $\pm$ s.e.m. in figures. Repeated measures analysis of variance was used to assess the effect of treatment on SBP. One-way analysis of variance, followed by *post hoc* testing using least significant difference, was used to evaluate differences in continuous variables, such as albumin excretion, among groups. Results were confirmed using non-parametric tests. Histological injury scores were compared using χ^2 testing. All tests were two-tailed and a $P<0.05$ was considered statistically significant.

ACKNOWLEDGMENTS

We are grateful to Ellen Donnert for her technical assistance in processing mouse tissues. Aldosterone concentrations were measured in the Vanderbilt Mouse Metabolic Phenotyping Center Hormone Assay Core, while echocardiograms were performed in the Murine Cardiovascular Core. This work was supported by NIH Grants HL67308, HL60906, DK56942, DK44757, and GM07569. Dr Ma was supported by grants from the Ministry of Education of China (EYTP) and the National Natural Science Foundation of China (30200125).

REFERENCES

1. Ambroisine ML, Milliez P, Nehme J *et al.* Aldosterone and anti-aldosterone effects in cardiovascular diseases and diabetic nephropathy. *Diabetes Metab* 2004; **30**: 311–318.
2. Greene EL, Kren S, Hostetter TH. Role of aldosterone in the remnant kidney model in the rat. *J Clin Invest* 1996; **98**: 1063–1068.
3. Fiebeler A, Schmidt F, Muller DN *et al.* Mineralocorticoid receptor affects AP-1 and nuclear factor-kappab activation in angiotensin II-induced cardiac injury. *Hypertension* 2001; **37**: 787–793.
4. Rocha R, Martin-Berger CL, Yang P *et al.* Selective aldosterone blockade prevents angiotensin II/salt-induced vascular inflammation in the rat heart. *Endocrinology* 2002; **143**: 4828–4836.
5. Pitt B, Zannad F, Remme WJ *et al.* The effect of spironolactone on morbidity and mortality in patients with severe heart failure. *N Engl J Med* 1999; **341**: 709–717.
6. Pitt B, Remme W, Zannad F *et al.* Eplerenone, a selective aldosterone blocker, in patients with left ventricular dysfunction after myocardial infarction. *N Engl J Med* 2003; **348**: 1309.
7. Farquharson CA, Struthers AD. Spironolactone increases nitric oxide bioactivity, improves endothelial vasodilator dysfunction, and suppresses vascular angiotensin I/angiotensin II conversion in patients with chronic heart failure. *Circulation* 2000; **101**: 594–597.
8. Zannad F, Alla F, Dousset B *et al.* Limitation of excessive extracellular matrix turnover may contribute to survival benefit of spironolactone therapy in patients with congestive heart failure: insights from the randomized aldactone evaluation study (RALES). Rales Investigators. *Circulation* 2000; **102**: 2700–2706.
9. White WB, Duprez D, St Hillaire R *et al.* Effects of the selective aldosterone blocker eplerenone versus the calcium antagonist amlodipine in systolic hypertension. *Hypertension* 2003; **41**: 1021–1026.
10. Sato A, Hayashi K, Naruse M, Saruta T. Effectiveness of aldosterone blockade in patients with diabetic nephropathy. *Hypertension* 2003; **41**: 64–68.
11. Pitt B, Reichek N, Willenbrock R *et al.* Effects of eplerenone, enalapril, and eplerenone/enalapril in patients with essential hypertension and left ventricular hypertrophy: the 4E-left ventricular hypertrophy study. *Circulation* 2003; **108**: 1831–1838.
12. Williams GH, Burgess E, Kolloch RE *et al.* Efficacy of eplerenone versus enalapril as monotherapy in systemic hypertension. *Am J Cardiol* 2004; **93**: 990–996.
13. Rachmani R, Slavachevsky I, Amit M *et al.* The effect of spironolactone, cilazapril and their combination on albuminuria in patients with hypertension and diabetic nephropathy is independent of blood pressure reduction: a randomized controlled study. *Diabet Med* 2004; **21**: 471–475.
14. Brilla CG, Matsubara LS, Weber KT. Anti-aldosterone treatment and the prevention of myocardial fibrosis in primary and secondary hyperaldosteronism. *J Mol Cell Cardiol* 1993; **25**: 563–575.

15. Young M, Fullerton M, Dilley R, Funder J. Mineralocorticoids, hypertension, and cardiac fibrosis. *J Clin Invest* 1994; **93**: 2578–2583.
16. Robert V, Silvestre JS, Charlemagne D *et al.* Biological determinants of aldosterone-induced cardiac fibrosis in rats. *Hypertension* 1995; **26**: 971–978.
17. Rocha R, Stier CTJ, Kifor I *et al.* Aldosterone: a mediator of myocardial necrosis and renal arteriopathy. *Endocrinology* 2000; **141**: 3871–3878.
18. Blasi ER, Rocha R, Rudolph AE *et al.* Aldosterone/salt induces renal inflammation and fibrosis in hypertensive rats. *Kidney Int* 2003; **63**: 1791–1800.
19. Zhou X, Ono H, Ono Y, Frohlich ED. Aldosterone antagonism ameliorates proteinuria and nephrosclerosis independent of glomerular dynamics in L-NAME/SHR model. *Am J Nephrol* 2004; **24**: 242–249.
20. Brown NJ, Kim KS, Chen YQ *et al.* Synergistic effect of adrenal steroids and angiotensin II on plasminogen activator inhibitor-1 production. *J Clin Endocrinol Metab* 2000; **85**: 336–344.
21. Calo LA, Zaghetto F, Pagnin E *et al.* Effect of aldosterone and glycyrrhetinic acid on the protein expression of PAI-1 and p22(phox) in human mononuclear leukocytes. *J Clin Endocrinol Metab* 2004; **89**: 1973–1976.
22. Oestreicher EM, Martinez-Vasquez D, Stone JR *et al.* Aldosterone and not plasminogen activator inhibitor-1 is a critical mediator of early angiotensin II/NG-nitro-L-arginine methyl ester-induced myocardial injury. *Circulation* 2003; **108**: 2517–2523.
23. Brown NJ, Nakamura S, Ma L-J *et al.* Aldosterone modulates plasminogen activator inhibitor-1 and glomerulosclerosis *in vivo*. *Kidney Int* 2000; **58**: 1219–1227.
24. Fujisawa G, Okada K, Muto S *et al.* Spironolactone prevents early renal injury in streptozotocin-induced diabetic rats. *Kidney Int* 2004; **66**: 1493–1502.
25. Loskutoff DJ, Quigley JP. PAI-1, fibrosis, and the elusive provisional fibrin matrix. *J Clin Invest* 2000; **106**: 1441–1443.
26. Eitzman DT, McCoy RD, Zheng X *et al.* Bleomycin-induced pulmonary fibrosis in transgenic mice that either lack or overexpress the murine plasminogen activator inhibitor-1 gene. *J Clin Invest* 1996; **97**: 232–237.
27. Kaikita K, Fogo AB, Ma L-J *et al.* Plasminogen activator inhibitor-1 deficiency prevents hypertension and vascular fibrosis in response to chronic nitric oxide synthase inhibition. *Circulation* 2001; **104**: 839–844.
28. Oda T, Jung YO, Kim HS *et al.* PAI-1 deficiency attenuates the fibrogenic response to ureteral obstruction. *Kidney Int* 2001; **60**: 587–596.
29. Eddy AA. Plasminogen activator inhibitor-1 and the kidney. *Am J Physiol Renal Physiol* 2002; **283**: F209–F220.
30. Kitching AR, Kong YZ, Huang XR *et al.* Plasminogen activator inhibitor-1 is a significant determinant of renal injury in experimental crescentic glomerulonephritis. *J Am Soc Nephrol* 2003; **14**: 1487–1495.
31. Huang Y, Haraguchi M, Lawrence DA *et al.* A mutant, noninhibitory plasminogen activator inhibitor type 1 decreases matrix accumulation in experimental glomerulonephritis. *J Clin Invest* 2003; **112**: 379–388.
32. Nicholas SB, Aguiniga E, Ren Y *et al.* Plasminogen activator inhibitor-1 deficiency retards diabetic nephropathy. *Kidney Int* 2005; **67**: 1297–1307.
33. Wang XY, Masilamani S, Nielsen J *et al.* The renal thiazide-sensitive Na-Cl cotransporter as mediator of the aldosterone-escape phenomenon. *J Clin Invest* 2001; **108**: 215–222.
34. Le Menuet D, Isnard R, Bichara M *et al.* Alteration of cardiac and renal functions in transgenic mice overexpressing human mineralocorticoid receptor. *J Biol Chem* 2001; **276**: 38911–38920.
35. Carvalho RS, Kostenuik PJ, Salih E *et al.* Selective adhesion of osteoblastic cells to different integrin ligands induces osteopontin gene expression. *Matrix Biol* 2003; **22**: 241–249.
36. Ma LJ, Yang H, Gaspert A *et al.* Transforming growth factor-beta-dependent and -independent pathways of induction of tubulointerstitial fibrosis in beta6(−/−) mice. *Am J Pathol* 2003; **163**: 1261–1273.
37. Kagami S, Border WA, Miller DE, Noble NA. Angiotensin II stimulates extracellular matrix protein synthesis through induction of transforming growth factor-beta expression in rat glomerular mesangial cells. *J Clin Invest* 1994; **93**: 2431–2477.
38. Lyons RM, Gentry LE, Purchio AF, Moses HL. Mechanism of activation of latent recombinant transforming growth factor beta 1 by plasmin. *J Cell Biol* 1990; **110**: 1361–1367.
39. Hertig A, Berrou J, Allory Y *et al.* Type 1 plasminogen activator inhibitor deficiency aggravates the course of experimental glomerulonephritis through overactivation of transforming growth factor beta. *FASEB J* 2003; **17**: 1904–1906.
40. Lim JY, Park SJ, Hwang HY *et al.* TGF-beta1 induces cardiac hypertrophic responses via PKC-dependent ATF-2 activation. *J Mol Cell Cardiol* 2005; **39**: 627–636.
41. Wang Q, Clement S, Gabbiani G *et al.* Chronic hyperaldosteronism in a transgenic mouse model fails to induce cardiac remodeling and fibrosis under normal salt diet. *Am J Physiol Renal Physiol* 2004; **286**: F1178–F1184.
42. Lacolley P, Labat C, Pujol A *et al.* Increased carotid wall elastic modulus and fibronectin in aldosterone-salt-treated rats: effects of eplerenone. *Circulation* 2002; **106**: 2848–2853.
43. Robert V, Heymes C, Silvestre JS *et al.* Angiotensin AT1 receptor subtype as a cardiac target of aldosterone: role in aldosterone-salt-induced fibrosis. *Hypertension* 1999; **33**: 981–986.
44. Wang Q, Hummler E, Nussberger J *et al.* Blood pressure, cardiac, and renal responses to salt and deoxycorticosterone acetate in mice: role of renin genes. *J Am Soc Nephrol* 2002; **13**: 1509–1516.
45. Cassis LA, Huang J, Gong MC, Daugherty A. Role of metabolism and receptor responsiveness in the attenuated responses to Angiotensin II in mice compared to rats. *Regul Pept* 2004; **117**: 107–116.
46. Weisberg AD, Albornoz F, Griffin JP *et al.* Pharmacological inhibition and genetic deficiency of plasminogen activator inhibitor-1 attenuates angiotensin II/salt-induced aortic remodeling. *Arterioscler Thromb Vasc Biol* 2005; **25**: 365–371.
47. Stefansson S, Lawrence DA. Old dogs and new tricks: proteases, inhibitors, and cell migration. *Sci STKE* 2003; **189**: e24.
48. Moriwaki H, Stempien-Otero A, Kremen M *et al.* Overexpression of urokinase by macrophages or deficiency of plasminogen activator inhibitor type 1 causes cardiac fibrosis in mice. *Circ Res* 2004; **95**: 637–644.
49. Ma LJ, Mao SL, Taylor KL *et al.* Prevention of obesity and insulin resistance in mice lacking plasminogen activator inhibitor 1. *Diabetes* 2004; **53**: 336–346.
50. Gardner H, Broberg A, Pozzi A *et al.* Absence of integrin alpha1beta1 in the mouse causes loss of feedback regulation of collagen synthesis in normal and wounded dermis. *J Cell Sci* 1999; **112**(Part 3): 263–272.
51. Rottman JN, Ni G, Khoo M *et al.* Temporal changes in ventricular function assessed echocardiographically in conscious and anesthetized mice. *J Am Soc Echocardiogr* 2003; **16**: 1150–1157.
52. Livak KJ, Schmittgen TD. Analysis of relative gene expression data using real-time quantitative PCR and the 2(-Delta Delta C(T)) method. *Methods* 2001; **25**: 402–408.